

Tunable Liquid Optics: Electrowetting-Controlled Liquid Mirrors Based on Self-Assembled Janus Tiles

Michael A. Bucaro,[†] Paul R. Kolodner,[‡] J. Ashley Taylor,[§] Alex Sidorenko,^{||} Joanna Aizenberg,[†] and Tom N. Krupenkin^{*,§}

School of Engineering and Applied Sciences, Harvard University, 29 Oxford Street, Cambridge, Massachusetts 01239, Bell Laboratories, 600 Mountain Avenue, Murray Hill, New Jersey 07974-0636, Department of Mechanical Engineering, University of Wisconsin, 1513 University Avenue, Madison, Wisconsin 53706-1572, and Department of Chemistry & Biochemistry, University of the Sciences in Philadelphia, 600 South 43rd Street, Philadelphia, Pennsylvania 19104-4495

Received October 23, 2008. Revised Manuscript Received November 25, 2008

In this paper, we describe a tunable, high-reflectivity optofluidic device based on self-assembly of anisotropically functionalized hexagonal micromirrors (Janus tiles) on the surface of an oil droplet to create a concave liquid mirror. The liquid mirror is deposited on a patterned transparent electrode that allows the focal length and axial position to be electrically controlled. The mirror is mechanically robust and retains its integrity even at high levels of vibrational excitation of the interface. The use of reflection instead of refraction overcomes the limited available refractive-index contrast between pairs of density-matched liquids, allowing stronger focusing than is possible for a liquid lens of the same geometry. This approach is compatible with optical instruments that could provide novel functionality—for example, a dynamic 3D projector, i.e., a light source which can scan an image onto a moving, nonplanar focal surface. Janus tiles with complex optical properties can be manufactured using our approach, thus potentially enabling a wide range of novel optical elements.

The emerging field of optofluidics^{1–5} exploits novel mechanisms for the manipulation of light—switching, focusing, image processing—based on the interaction of light beams with optical elements made of liquids. One simple but powerful optofluidic device is the liquid lens,^{5–10} whose basis is the spherical shape of liquid droplets. The shape of a liquid lens—and therefore its focal length—can be controlled by a variety of techniques, such as electrowetting,^{1,2,7} variation of hydrostatic pressure,^{8,9} and exposure to environmental changes.¹⁰ However, turning this simple concept into a reliable device presents many practical challenges. For example, to resist shock, vibration, and distortion by gravity, a microlens must be formed by the interface between two immiscible, density-matched liquids. The refractive-index contrast between such pairs of liquids is limited, and their optical dispersions must also be in the proper ratio to minimize chromatic aberrations.^{1,2} One of the ways to mitigate this problem is to enhance the optical properties of the liquid–liquid interface by covering it with optically active solid particles. These considerations led us to conceive of a reflective element consisting of a liquid lens whose refracting surface is covered with reflective tiles to form a “liquid mirror”. In such a device, the intrinsic

optical properties of the liquid–liquid interface are of secondary importance.

Large-scale liquid mirrors have long been a subject of interest to astronomers. The classic astronomical liquid mirror consists of a pool of liquid metal which is slowly rotated to produce a parabolic reflecting surface that serves as the primary mirror of a vertically oriented, azimuth-scanning telescope.^{11,12} To avoid such problems as large mass and the limited usable temperature range of liquid metals, researchers have turned to other flexible reflecting surfaces, such as nanometer-sized colloidal silver particles deposited from a suspension onto the top surface of a thin layer of low-density oil,^{13,14} as well as simple evaporation of a metal film onto the surface of a low-vapor-pressure ionic liquid¹⁵ suitable for deployment on the surface of the moon. A parallel thread of development focuses on small-area, tunable liquid mirrors for use in adaptive optics.^{16,17} The fabrication techniques described in refs 13–17 are well-suited for making high-reflectivity, low-scatter liquid mirrors. They have been employed to fabricate first-surface mirrors with weak curvature, with apertures ranging from a few centimeters to several meters.

Our interest is in the complementary domain of small, packaged optical elements with strong curvature, to be used for focusing or scanning millimeter-sized light beams. Nanometer-scale colloidal metal particles, which aggregate to the interface between two immiscible liquids, could be used to fabricate such mirrors.

* To whom correspondence should be addressed. E-mail: tnk@engr.wisc.edu.

[†] Harvard University.

[‡] Bell Laboratories.

[§] University of Wisconsin.

^{||} University of the Sciences in Philadelphia.

(1) Kuiper, S.; Hendriks, B. H. W. *Appl. Phys. Lett.* **2004**, *85*, 1128.

(2) Krogmann, F.; Mönch, W.; Zappe, H. J. *Opt. A: Pure Appl. Opt.* **2006**, *8*, S330.

(3) Monat, C.; Domachuk, P.; Eggleton, B. J. *Nat. Photon.* **2007**, *1*, 106.

(4) Psaltis, D.; Quake, S. R.; Yang, C. *Nature* **2006**, *44*, 381.

(5) Levy, U.; Shamaï, R. *Microfluid Nanofluid* **2008**, *4*, 97.

(6) Commander, L. G.; Day, S. E.; Selviah, D. R. *Opt. Commun.* **2000**, *177*, 157.

(7) Krupenkin, T.; Yang, S.; Mach, P. *Appl. Phys. Lett.* **2003**, *82*, 316.

(8) Werber, A.; Zappe, H. *Appl. Opt.* **2005**, *44*, 3238.

(9) Wang, W.; Fang, J.; Varshney, K. *IEEE Phot. Tech. Lett.* **2005**, *17*, 2643.

(10) Dong, L.; Agarwall, A. K.; Beebe, D. J.; Jiang, H. *Nature* **2006**, *442*, 551.

(11) Tremblay, G.; Borra, E. F. *Appl. Opt.* **2000**, *39*, 5651.

(12) Hickson, P.; Frommer, T.; Cabanac, R.; Crofts, A.; Johnson, B.; de Lapparent, V.; Lanzetta, K. M.; Gromoll, S.; Mulrooney, M. K.; Sivanandam, S.; Truax, B. *Publ. Astron. Soc. Pacif.* **2007**, *119*, 444.

(13) Borra, E. F.; Ritcey, A. M.; Bergamasco, R.; Laird, P.; Gingras, J.; Dallaire, M.; da Silva, L.; Yockell-Lelièvre, H. *Astron. Astrophys.* **2004**, *419*, 777.

(14) Gingras, J.; Déry, J.-P.; Yockell-Lelièvre, H.; Borra, E. F.; Ritcey, A. *Colloids Surf. A* **2006**, *279*, 79.

(15) Borra, E. F.; Seddikil, O.; Angel, R.; Eisenstein, D.; Hickson, P.; Seddon, K. R.; Worden, S. P. *Nature* **2007**, *447*, 979.

(16) Truong, L.; Borra, E. F.; Bergamasco, R.; Caron, N.; Laird, P.; Ritcey, A. *Appl. Opt.* **2005**, *44*, 1595.

(17) Laird, P.; Caron, N.; Rioux, M.; Borra, E. F.; Ritcey, A. *Appl. Opt.* **2006**, *45*, 3495.

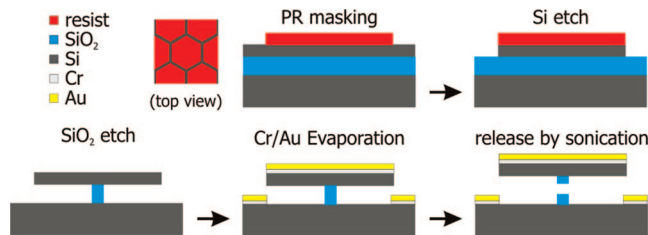


Figure 1. Micromirror fabrication. Hexagonal, gold-coated Si mirrors are produced using standard lithographic and dry-etching techniques. Partial dissolution of the underlying SiO₂ layer leaves the micromirrors attached to the substrate by weak stalks which can be fractured by sonication.

However, the transition to more complex optical function is difficult since subwavelength particles can provide only very basic optical effects such as uniform scattering or reflection. The approach we have taken explicitly relies on the use of reflective particles which are much larger than a wavelength. These micromirrors can be lithographically patterned as diffraction gratings or microlenses as well as reflectors, and they can even include active devices. These possibilities open up a wide new domain of previously unavailable, tunable optical elements.

The micromirrors used in this work are silicon hexagons of diameter 8 μm and thickness 1 μm . They are coated with a thin layer of gold on one face, and differential chemical functionalization of the gold and bare faces is used to create a strong anisotropy in wettability, with the gold side substantially more hydrophobic than the bare face. When released into an oil droplet which is deposited onto an aqueous subphase, these “Janus tiles” sediment to the liquid–liquid interface, where they align parallel to the interface, with the gold surfaces facing the oil, thus forming a concave gold mirror. By contacting the top of the oil droplet to an insulated, transparent, electrically conducting glass slide and applying a voltage between the substrate and the aqueous subphase, we can change the shape of the mirror by electrowetting, thus tuning its focal length.

“Janus particles”—small particles with anisotropic surface properties—have been fabricated using a number of different techniques.^{18–21} Recently, Walther et al.²² have described the production of “Janus discs”: flat particles whose opposite faces are composed of different polymers. These Janus discs were not specifically designed to be reflective, and their small size (typically hundreds of nanometers) and wide size distribution render them unsuitable for our goal of fabricating reproducible micromirrors.

For the production of large numbers of identical “Janus tiles”, we turned to photolithographic techniques.²³ Silicon-on-insulator (SOI) wafers (1 μm Si with a 0.4 μm buried SiO₂ layer) were processed using standard deep-UV lithography (248 nm) and dry reactive ion etching (DRIE) to produce 8 μm diameter, 1 μm thick silicon hexagons (Figure 1). After DRIE, the wafers were treated with 5% hydrofluoric acid, leaving an approximately 1 μm diameter SiO₂ stalk attaching the mirrors to the underlying silicon substrate. This fragile attachment allows the mirrors to be subsequently separated from the substrate by sonication.

(18) Casagrande, C.; Fabre, P.; Raphaël, E.; Veyssié, M. *Europhys. Lett.* **1989**, *9*, 251.

(19) Glaser, N.; Adams, D. J.; Böker, A.; Krausch, G. *Langmuir* **2006**, *22*, 5227.

(20) Shepherd, R. F.; Conrad, J. C.; Rhodes, S. K.; Link, D. R.; Marquez, M.; Weitz, D. A.; Lewis, J. A. *Langmuir* **2006**, *22*, 8618.

(21) Dendukuri, D.; Pregibon, D. C.; Collins, J.; Hatton, T. A.; Doyle, P. S. *Nat. Mater.* **2006**, *5*, 365.

(22) Walther, A.; André, X.; Dreschler, M.; Abetz, V.; Müller, A. H. E. *J. Am. Chem. Soc.* **2007**, *129*, 61876198.

(23) Brown, A. B. D.; Smith, C. G.; Rennie, A. R. *Phys. Rev. E* **2000**, *62*, 951.

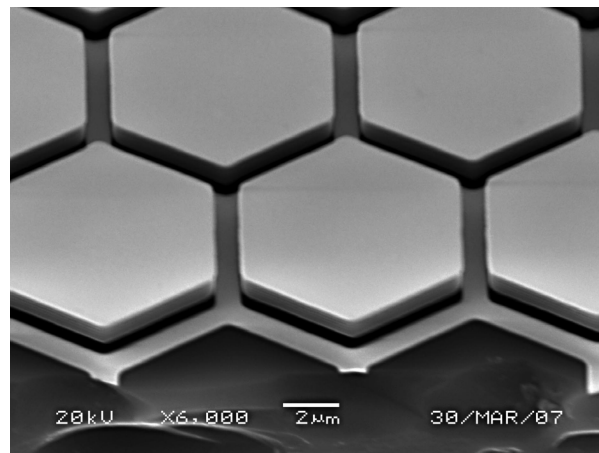


Figure 2. SEM image of unreleased micromirrors. The hexagonal structures are the micromirrors after etching and Cr/Au deposition. A shadowing of the Cr/Au deposition is visible as a 1 μm wide lattice on the substrate. The 1 μm SiO₂ stalks connecting the mirrors to the substrate are not visible. Scale bar is 2 μm .

A 7 nm Cr adhesion layer and a subsequent 100 nm Au reflecting layer were then deposited by e-beam evaporation. The wafers were then diced and treated with a base piranha etch solution (1:1:1 NH₄OH:30% H₂O₂:diH₂O) for 15 min. For some experiments, standard methods were used to create self-assembled monolayers (SAMs) of an organothiol and/or an organosilane to modify the surface energies of the gold and silicon faces, respectively. Figure 2 shows an SEM photograph of micromirrors still attached to the substrate.

Micromirrors were released into 500 μL of oil by sonication in a glass cuvette, and a droplet of the micromirror suspension was then deposited onto the surface of water in a glass Petri dish (Figure 3A). Over the course of several minutes, the micromirrors sedimented onto to the oil–water interface and self-assembled into a liquid mirror, with the gold faces facing predominantly toward the oil phase because of the different wetting properties of the two faces (Figure 3B). Liquid mirrors were created using oils with moderately high interfacial tensions with water and near unit specific gravity. These included decane, silicone oil PDM7040, benzyl benzoate, and pentyl benzoate (specific gravity $\rho_{25} = 0.984$, surface tension $\sigma_{25} = 33$ mN/m, refractive index $n_{20}^D = 1.495$, avg. molar extinction 400–700 nm = 0.0021 L/mol·cm). The quality of the liquid mirrors with regard to reflectivity and alignment of the micromirrors with the interface was observed to be best using pentyl benzoate, which was used in all subsequent studies. To produce floating mirrors of different curvatures, isopropanol (1–20% v/v) was added to the aqueous phase to reduce its interfacial tension. After removal of excess oil, the micromirrors were observed to be densely packed, covering 90% of the interface (Figure 3C). The percentage of mirrors in the proper orientation (gold face toward oil) was approximately 80%. In some cases, the oriented fraction was marginally lower but improved overnight or with sonication. The coplanar alignment of the micromirrors with the liquid–liquid interface is evidenced by sharp reflected images of the liquid mirrors (Figure 3D).

To evaluate the dynamic stability of the liquid mirrors, free-floating mirrors were excited acoustically at 19 Hz to produce resonant vibrational modes which dramatically distorted their shape. Frame captures of a video are shown in Figures 3E, F, and G. The videos demonstrate that the reflective surfaces remain intact, with the micromirrors attached to the oil–water interface,

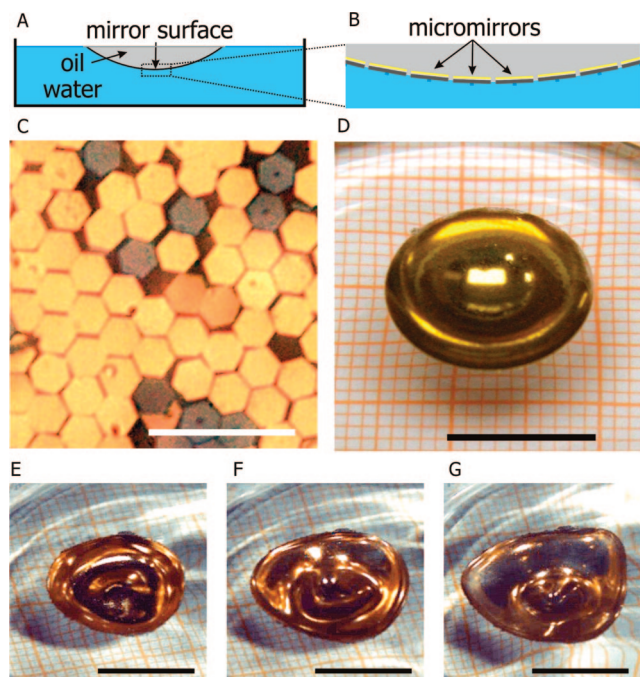


Figure 3. Self-assembled liquid mirror and micromirror organization. (A) A droplet of oil containing micromirrors in suspension is floated on a water surface. (B) The micromirrors assemble at the oil–water interface with the gold face oriented toward the oil phase. (C) This orientation is preferred due to the relative surface energies of the gold and silicon faces, although not all micromirrors orient as desired. Remnants of the SiO₂ stalks can be seen on the silicon faces at the top right corner of the image. (D) The micromirror assembly creates a mirror with the curvature of the oil–water interface. (E, F, G) Frame captures (450 ms between frames) of an acoustically excited liquid mirror. The mirror remains intact and fully reflective while undergoing large dynamic changes in the shape of the oil–water interface. Scale bars: (C) 25 μm , (D, E, F, G) 1 cm.

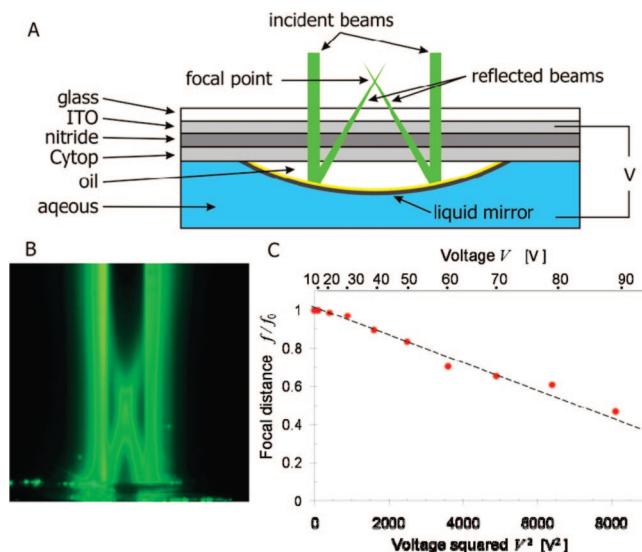


Figure 4. Dynamic control of curvature by electrowetting. (A) Diagram of a liquid mirror integrated with an electrowetting substrate and the optical path for measurement of the mirror's focal distance. (B) Video frame showing the laser beam path used to measure the focal distance. (C) Graph of the relative focal distance f/f_0 as a function of voltage (V) and voltage square (V^2). The value of f_0 is approximately 8.3 mm. Dashed line is to guide the eye only.

and exhibit continuous sharp reflectivity while undergoing large dynamic deformations (video provided in Supporting Information).

The focal length of liquid mirrors was controlled using electrowetting (Figure 4). Transparent, conducting substrates for these experiments were fabricated from indium-tin-oxide (ITO)-coated float glass (Delta Technologies, Stillwater, MN) that was electrically insulated by deposition of 300 nm of SiN_x by plasma-enhanced chemical vapor deposition.

An approximately 0.5 μm thick layer of fluorinated polymer (Cytop CTL-809M, Asahi Glass Co., Japan) was then spin-coated (10 s at 4000 rpm) onto the substrate and cured (1 h at 40 $^{\circ}\text{C}$, followed by 3 h at 200 $^{\circ}\text{C}$) to produce a hydrophobic surface and minimize contact-angle hysteresis. The substrate was gently lowered onto the surface of the liquid mirror until it made contact with both the oil and water surfaces (Figure 4A). The focusing properties of the mirror were visualized by illumination with a broad 532 nm laser beam which was centrally masked to produce parallel incident light beams. These were rendered visible by a fluorophore solution (Rhodamine 6G in ethanol) contained in a cuvette resting on top of the electrowetting substrate (Figure 4B). Voltage was applied between the conducting layer of the substrate and a Pt wire electrode in contact with the aqueous subphase (15% propanol, 15 mM NaCl). Increasing the voltage between the ITO layer and the water resulted in retraction of the liquid mirror circumference and an increase in its curvature.

The micromirror focal length f is determined by the contact angle θ formed by the water–oil interface with the ITO glass surface, according to the formula⁷

$$f^3 = \frac{3\Omega}{8\pi(1 - \cos\theta)(2 - \cos^2\theta - \cos\theta)} \quad (1)$$

where Ω is the oil droplet volume. The dependence of the contact angle θ on applied voltage V follows from the classical electrowetting equation⁷ modified to account for the fact that the contact angle θ in our case is measured from the oil side rather than from the water side of the interface, thus leading to an increase of θ with applied voltage

$$\cos\theta(V) = \cos\theta_0 - \frac{\epsilon_0\epsilon_r}{2d\gamma_{wo}}V^2 \quad (2)$$

Here, V is the applied voltage; θ_0 is the initial contact angle at 0 V; γ_{wo} is the water–oil interface energy per unit area; ϵ_r is the permittivity of the dielectric insulator; ϵ_0 is the permittivity of vacuum; and d is the dielectric thickness. From eqs 1 and 2, one can see that the Taylor expansion of f with respect to V takes the form $f = \sum_{i=0}^{\infty} a_i V^{2i}$, where the coefficients a_i are functions of θ_0 , γ_{wo} , ϵ_r , and d . For voltages small enough to cause only a modest variation of the contact angle, the first two terms dominate, leading to an approximately linear relationship between f and V^2 .

The change in mirror curvature as a function of voltage was measured using optical images of the beams reflected from the mirror surface and is shown in Figure 4C as a function of voltage (V) and voltage squared (V^2). As predicted by theory, f is indeed approximately linear in V^2 . The voltage response of the liquid mirror resulted in a 2-fold focal-distance range. It should be noted that the demonstrated tunability range and response time do not represent intrinsic limitations of the device performance. Since the strength of the electrowetting phenomenon is inversely proportional to the film thickness, reducing the thickness of the dielectric from nearly 1 μm in our demonstration to approximately 100 nm using modern semiconductor processing techniques would lead to an order of magnitude increase in sensitivity. Similarly, response time, which was on the order of 100 ms in this demonstration, is dependent on the mirror size and was previously shown to approach several milliseconds in millimeter-diameter

liquid lenses controlled by electrowetting.⁷ Reflectivity of the liquid mirror is determined by the efficiency of transmission through the oil phase, the micromirror surface reflectivity, and the packing density of the oriented micromirrors. In this demonstration, strong reflectivity was maintained during deformation of the mirror, and no change in the packing density of the mirrors was observed.

The approach explored in this work can enable a wide range of new optofluidic devices. Combining the axial focus control presented here with the lateral scanning capability described previously⁷ would allow us to make a projector, in which a point source of light is converted by the concave liquid mirror into a collimated beam which can be scanned over a wide angle in space. Since the liquid micromirror can continuously change its focus as it scans the beam, sharp projection to strongly curved or even moving surfaces can be accomplished. Patterning the micromirrors as diffraction gratings would allow the liquid mirror to bring a collimated input beam of white light to a wavelength-dependent focus, thus turning the mirror into a source of tunable, narrow-band light. This can enable a compact multiprimary color projector capable of enhancing the image color gamut using the exceptionally broad range of colors generated by the diffraction grating. Using tiles with active elements, which could derive power from a potential difference applied between the two

immiscible fluids, could further expand the functionality of the proposed optofluidic devices. For example, each tile could contain an LED and a collimating microlens and be oriented with the output beam emitted from the convex face of the liquid mirror. The resulting fan of output beams can illuminate a wide solid angle with poor uniformity (at high curvature) or a narrower solid angle with high uniformity (at low curvature). Replacing the LEDs with detectors turns this structure into a compound “fly’s eye”²⁴ in which electrical tuning allows a tradeoff between spatial resolution and field of view.

Acknowledgment. We thank Ben Hatton, Evelyn Wang, and Todd Salamon for enlightening discussions and technical assistance. Also appreciated was the processing support from the New Jersey Nanotechnology Consortium.

Supporting Information Available: Videos demonstrating that the reflective surfaces remain intact, with the micromirrors attached to the oil–water interface, and exhibiting continuous sharp reflectivity while undergoing large dynamic deformations. This material is available free of charge via the Internet at <http://pubs.acs.org>.

LA803537V

(24) Brückner, A.; Duparré, J.; Dannberg, P.; Bräuer, A.; Tünnermann, A. *Opt. Express* **2007**, *15*, 11922.